# Ground Deformation Monitoring of the Santorini Volcano using Satellite Radar Interferometry

E. Lagios [1], Is. Parcharidis [2], M. Foumelis [1] & V. Sakkas [1]

[1] *National Kapodistrian University of Athens, Space Applications Research Unit in Geosciences, Laboratory of Geophysics, Department of Geophysics & Geothermics, Panepistimiopolis - Ilissia, 157 84 Athens, Greece, lagios@geol.uoa.gr, mfoum@geol.uoa.gr, vsakkas@geol.uoa.gr*

[2] *Harokopio University, Departement of Geography, El. Venizelou 70, 176 71 Athens, Greece, parchar@hua.gr*

***Abstract*-The island complex of Santorini is located at the central part of the Hellenic Volcanic Arc in the Southern Aegean Sea. This volcano complex basically consists of five islands, Thera, Therassia, Palea Kammeni, Nea Kammeni and Aspronisi forming a caldera of 83 km$^2$ with 390m depth. The last significant volcanic activity took place between 1925 and 1950. However, the volcano is at a rest state during the last 50 years. The present work refers to the ground deformation monitoring of the area using ERS1, ERS2 and Envisat radar scenes from 1993 to 2004. A total number of four ERS1&2 SLC radar images covering the period 1993 to 1999, and two ENVISAT ASAR images for the period 2003-2004 were used. The method applied was the two-passes interferometry with a contribution of a high resolution Digital Elevation Model. The interferometric results show that although the volcano is at a rest phase, in the two volcanic centers of Palea and Nea Kammeni ground deformation (subsidence) of 62 mm along the line of sight of the satellite was detected.**

## I. Introduction

Volcano hazard monitoring and mitigation is based on techniques that provide information over two different time scales. Stratigraphic and geologic studies reveal a volcano's long-term eruptive history, while monitoring shallow seismicity and ground deformation typically documents short-term activity.

Techniques like tiltmeters and Differential GPS are used to measure the ground deformation in the volcanoes. However, these techniques provide point coverage, since they are detecting changes at single points (stations) on the ground surface. The amplitude and the direction of the vector movement of these points enable scientist to piece together the general pattern of ground deformation, but fail to detect small-local scale movements due to limitations on the number of the ground stations.

The critical information gained through geologic mapping in volcanic centers, from local field studies, represent static documents that need to be updated and modified as new data and knowledge is acquired.

Space based geodetic techniques may extend the warning time before eruptions to years or even decades, filling a crucial gap between traditional volcano monitoring of shallow precursors (hours to months of warning) and the long-term volcano hazards assessments based on eruptive history.

Spaceborne radar interfrometry [1, 2] has already shown its ability in mapping ground deformation, like co-seismic deformation, as well as long-term movements as is the ground deformation in volcanoes, landslides and subsidence [3, 4, 5]. Geodetic techniques can be used to identify ground-surface deformation associated with movement of magma and/or hydrothermal fluids beneath volcanoes.

Repeat-pass SAR interferometry (InSAR) technique relies on the processing of two SAR images of the same portion of the Earth's surface obtained from slightly displaced passes of the SAR antenna at different times. InSAR measures deformation by mapping changes in the ground-to-satellite distance between two satellite images, producing an interferogram. The change in distance is shown using a repeating cycle of colors (each cycle is called a fringe), making a contour map of the displacement of the ground in the satellite look direction.

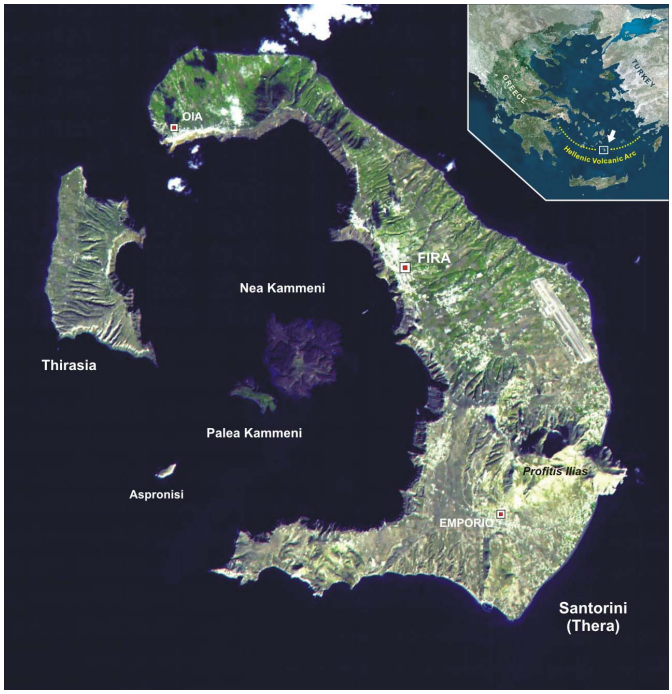


Fig. 1 Location map of the study area.

The flexibility of the differential InSAR procedure represents a fundamental factor for their applicability. SAR interferometry can monitor regional surface displacements with the advantage of covering large areas providing spatial coverage.

The present work is part of a research project in the framework of ESA's Announcement of Opportunity for Greece. The study aims to contribute to the better understanding of the magnitude, style and pattern of surface deformation of the complex of Santorini islands. This work aims to act as a basis for volcanic hazard assessment. Moreover the ability to monitor surface movements under volcanic rest conditions is demonstrated.

## II. Description Of Santorini Volcano

The island complex of Santorini (Thera) is located on the Hellenic Volcanic Arc (HVA), which stretches from Aegina and Methana in the west over Milos and Santorini and terminates at Kos and Nisyros in the east. The HVA is a result of northeastward-directed subduction (started around 4 Ma at the beginning of Pliocene) of the African plate beneath the Aegean microplate [6, 7, 8].

The Santorini volcanic complex is basically consisted of five islands: Thera, Therassia, Palea Kammeni, Nea Kammeni and Aspronisi, forming a caldera of 83 $km^2$ with 390m depth. The major islands of There and Therasia form a circular feature around a caldera, in which the post-caldera islands Palea and Nea Kameni are located. Analytical description of the caldera formation has been discussed in [9].

The morphology of the volcanic complex is determined by steep slopes in the inner part of the caldera escarpment that stands about 300m above the sea level. The highest point in the complex is located at the Profitis Ilias mountain (564m) at the SE of the capital city of Fira. The outer part of the complex, which comprise the vestigial part of the volcanic cone, maintain gentle slopes. The present morphology of Palea and Nea Kameni islands is a result of accumulation of successive lava flows during the period of paroxysmic activity at the Minoan Era. At that period (middle of the 11th century BC) a major eruption resulted in the destruction of the Minoan civilization.

The closest seismic source, according to historical and instrumental seismicity, is located at the center of the caldera structure by the activity of which it is related. The largest earthquake occurred around 100 km away, north of Amorgos island, with a magnitude of Mw=7,5.

Most recent eruption occurred in 1950, while present volcanic activity is restricted to the island of Palea and Nea Kammeni, mainly in a form of hydrothermal discharges. However, the seismic activity has decreased considerably since the big Minoan eruption 3500 years ago [10]. Detailed description of its main post-Minoan eruptive events could be found in [11].

As a result of the numerous eruptive events the largest part of the complex is covered by volcanic products (basalt to rhyolite) that belong to the calc-alkaline series. The volcano is dominated by andesitic and basaltic lava, unconsolidated pyroclastic deposits and volcanic ash [12-13]. The caldera cliffs exhibit well preserved sequence of lava and pyroclastic deposits of twelve major explosive eruptions during a period of 360000 years as well as dissected remains of ancient lava shields and lava domes. Alpine basement crop out at the area of high altitude at mountain of Profitis Ilias. It consists of HP/LT metamorphic phases (e.g. blue schists) and low grade metamorphic sedimentary sequence of carbonates, dolomites and flysch. Quaternary deposits are limited to some coastal sediments and debris cones formed by the collapse of unstable parts of the volcano without necessary accompanying eruptions.

## III. Data Used – Interferometric Processing

One of the basic parameters in the interferometric technique application is the selection of the proper scenes in order to create suitable interferometric pairs. For selecting suitable data the following criteria have been used:

(i) Perpendicular baseline (Bp) lower than 50 meters (for best results)
(ii) SAR and ASAR acquisitions of the same season to avoid seasonal land use changes affecting the coherence between the images forming an interfeormetric pair,
(iii) Time coverage of the ERS and Envisat.

The total number of scenes and their characteristics, selected for the application, are shown in table I. Six ERS 1 & 2 SAR scenes and two ERS-like Envisat ASAR (Is2) scenes were selected covering all of the Santorini volcano complex, in descending orbits. The scenes cover the period 1993 to 2003. The ability of a SAR-image pair to form an interferometric image to detect surface deformation is highly depended on the orbital separation. That is expressed with the baseline component perpendicular to radar LOS (Line-of-sight). Among the possible combinations, the analysis was restricted to those interferometric pairs having the shortest perpendicular baselines to limit geometric decorrelation [14] and topographic contribution [15]. The suitable interrferometric pairs are shown in table 2, where perpendicular baseline (Bp), altitude of ambiguity (ha) and time interval between each pair of the images are given. Except the Envisat pair the other two pairs show Bp lower than 10 meters and consequently high altitude of ambiguity values. The temporal separation between the scenes is relatively high increasing the possibility of low coherence. The meteorological conditions, provided by the Hellenic meteorological Service, were the appropriate one during the day of the acquisition. Although some pairs shows values of the baseline parameter that are acceptable, their processing did not yield satisfactory results, because the images are from different tracks of acquisition and the study area is imaged on a different geometry.

TABLE I

| Date | Mission | Orbit | Track | Frame |
|---|---|---|---|---|
| 20 Jun 1993 | ERS 1 | 10086 | 422 | 2871 |
| 26 May 1995 | ERS 2 | 505 | 150 | 2871 |
| 13 Jun 1995 | ERS 1 | 20450 | 422 | 2871 |
| 27 Sept 1996 | ERS 2 | 7519 | 150 | 2871 |
| 22 Oct 1999 | ERS 2 | 23551 | 150 | 2871 |
| 10 Nov 1999 | ERS 2 | 23823 | 422 | 2871 |
| 03 Sept 2003 | ENVISAT | 7898 | 2329 | 729 |
| 31 Mar 2004 | ENVISAT | 10904 | 2329 | 729 |

TABLE II

| Master | Slave | $B_p$ | $h_a$ | dt |
|---|---|---|---|---|
| 20 Jun 1993 | 13 Jun 1995 | 5,39 | 1745,06 | 724 |
| 26 May 1995 | 22 Oct 1999 | 7,98 | 1179,21 | 1611 |
| 03 Sept 2003 | 31 Mar 2004 | 111,05 | 84,79 | 211 |

The two-pass differential interferometry method (or DEM-elimination method) was applied. This method uses two SAR images to produce one interferogram. To perform the differential interferogram, another interferogram has to be created or synthesized. The synthesized interferogram is generated from an existing digital elevation model (DEM) of the area and then is subtracted from the original interferogram. Thereby removing all fringes that relate to ground elevation only fringes that represent surface displacements remain. The phase differences that remain as fringes in the differential interferogram are a result of range changes of any displaced point on the ground. In the differential interferometry, each fringe is directly related to the radar wavelength (56 mm for ERS and Envisat) and represents a displacement along the line of sight (LOS) of half the above wavelength (28 mm).

The interferometric process starts with a DEM generation of 20 meters resolution and height accuracy of about ±4m. The DEM was geocoded in Universal Transverse Mercator (UTM) projection (similar to the SAR and ASAR scenes), so that errors due to reprojection of the dataset to be eliminated. Such process does not yield artifacts in the deformation maps. The information contained in the produced DEM was used to remove the topographic component of the phase in the interferograms. In the following step, the initial orbit state vectors for ERS images have been downloaded from the Delft Institute (NL) for Earth-Oriented Space Research (DEOS). DEOS precise ERS orbits are based on the DGM-E04 gravity field model and the SLR and OPR2 altimeter crossovers and normal points [16].

The interferometric processing and analyses were based on the "Atlantis" software package. The main steps of the processing include, coregistration of the master and slave images, validation of the pair for spatial and spectral overlap, coregistration of the external DEM to master at a sub-pixel accuracy, "flat" earth phase removal, spectral filtering removal of elevation phase contribution using the external DEM, first interferogram production, coherence map generation, phase unwrapping using the Disk masking Algorithm, slant range change map generation and geocoding into UTM projection.

## IV. Results – Discussion

The differential images are highly depended on several factors, and as a consequence, the following should be considered in order to validate and interpret the obtained results:

i) Uncompensated topography, a differential interferogram is by definition processed in conjunction with a digital elevation model (DEM), such that the effects of topography are removed from the output phase image. The magnitude of topographically related phase errors is thus a function of the quality of the DEM (in this study a high resolution DEM was used the accuracy of which was evaluated), the accuracy with which it is co-registered to the data set, and the baseline. The 'altitude of ambiguity' parameter for a differential interferogram corresponds to the uncompensated topography necessary to cause one fringe cycle in the interferogram (fringe interval). With small baselines residual topographic phase effects are less significant. At higher baselines and in areas of mountainous relief the residual phase effects can become more apparent, of the order of a phase cycle. The interferometric pairs particularly those of ERS have low baselines and consequently present high altitude of ambiguity values, resulting small probabilities to have in the interferogram fringes related to the local topography.

ii) The RMS error of the coregistration between the SAR images and between the SAR master image and the external DEM. A high number of coregistration tie-points have been used with RMS less than one pixel.

iii) Quality of coherence: the temporal separation between the two acquisitions forming the pairs is relatively high. The latter could favor the temporal decorrelation. It is deduced form the coherence images that the Santorini and Thiressia islands show a fairly good coherence while the coherence over Palea and Nea Kammeni islands is constantly high, even for long temporal separations due to their land cover type (bare lavas).

iv) Possible atmospheric effects, regarding effects due to changes in properties of the atmosphere. According to the Hellenic Meteo Service the area was free of clouds during the days of acquisition and the day before. Additionally, the production of more than one interferogram over the area showing similar results is an extra indication that the fringes appeared in the interferograms correspond to real displacement and we consider that the fringes are mainly resulted from the ground deformation associated with the volcanic activity.

The evaluation and analysis for each of the three generated interferograms follows.

*June 1993 – June 1995 interferogram*

The obtained corregistration between the scenes using 24 tiepoints was 0,2 pixel, while the corregistration between the master scene and the DEM applying 14 ground control points

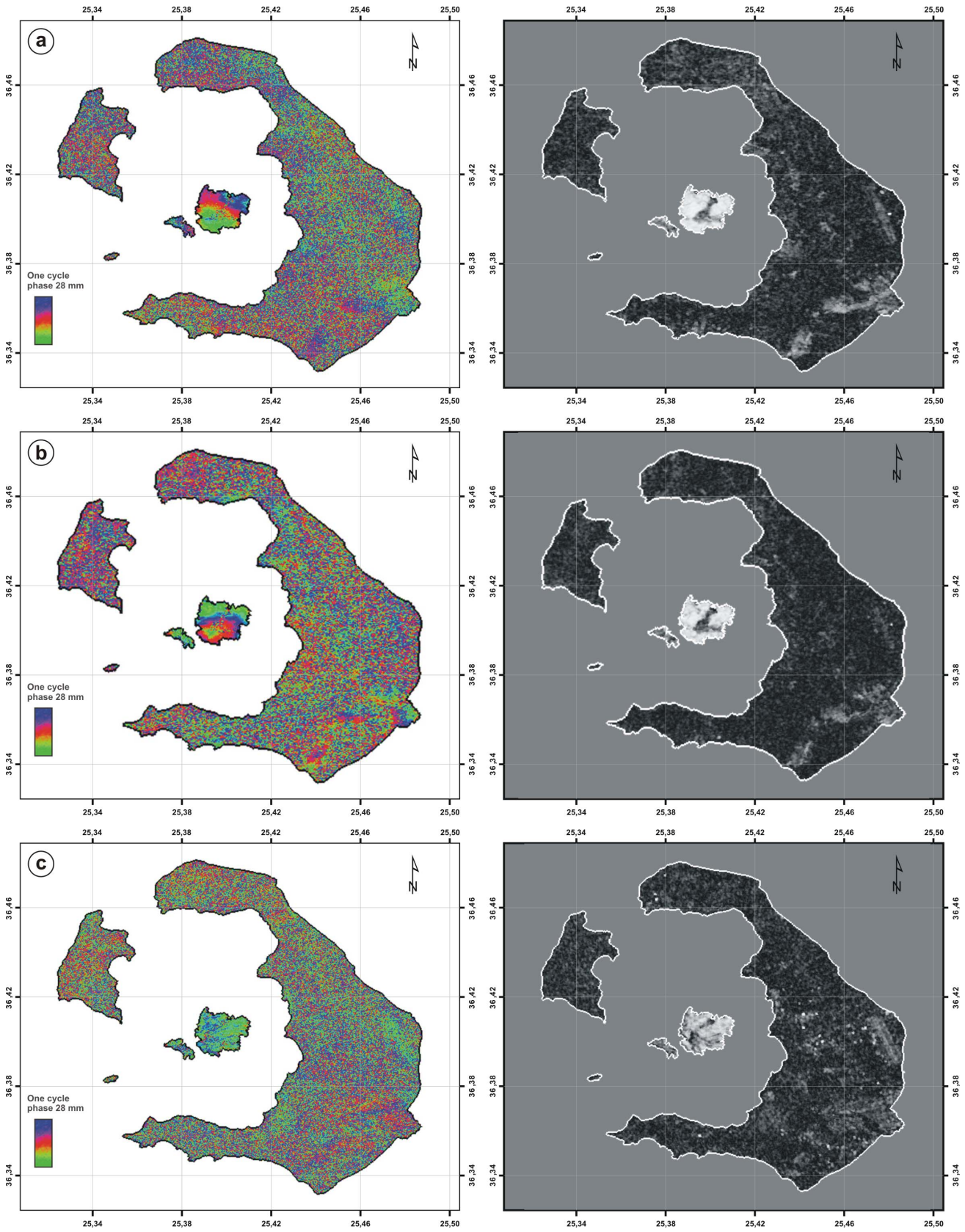


Fig. 2 Interferometric images (left column) and the corresponding coherence images (right column) for the periods, June 1993 – June 1995 (a), May 1995 – Oct. 1999 (b) and Sept. 2003 – Mar. 2004 (c).

(GCPs), well distributed through out the area of interest, was less than 0,9 pixel.

Although the land cover type is favorable to the method (semiarid with very sparse vegetation) and the acquisition of the scenes took place in the same month of the year, only the island of Nea Kammeni shows high coherence. The restof the islands of the volcanic complex show low coherence, with zones of medium coherence appear locally (Alpine outcrops in the southeastern part of Thera).

A significant indication of surface deformation at the area is recognized on the Nea Kammeni island. An almost full fringe pattern of deformation was detected at the Nea Kammeni Island.. indicating about 18 mm (LOS) of surface motion away from the sensor (positive phase value) with maximum of deformation point located in the southern central part of it. This could be interpreted as a downlift of the Nea Kammeni volcanic center. The calculated altitude of ambiguity (1745m) was far larger that the elevation of Nea Kammeni (125m), so that the detected change could not be attributed to topographic phase.

*May 1995 – October 1999 interferogram*

The error of corregistration obtained (around 0,9 pixel) was higher of that of the 1993-1995 interferogram, whereas the corregistration of DEM using 12 GCPs yield an error of less than 0,9 pixel. Despite the long time separation between the scenes the coherence image was almost similar to that of the 1993-1995. It seems that the largest temporal separation of the specific interferometric pair, does not affect at least in at the particular area of Nea Kammeni.

Maximum observed deformation shown as phase variations of just over one fringe equivalent to LOS range changes of about 44 mm, almost at the same location with the 1993-1995 interferogram. Due to small perpendicular baseline ($B_p$=7,89m) the altitude of ambiguity was ha=1179.21m, a fact that emphasize the pertinence of the observed movement. The characteristics of the movement are in total agreement with the observed at the 1993-1995 interferogram movement, implying the continuity of downlift (positive phase value) of the Nea Kammeni volcanic center at least until 1999.

*September 2003 – March 2004 interferogram*

Applying 31 tieponts for scene corregistration and 10 GCPs for DEM corregistration the obtained error was less than 0.3 pixel and 0,9 pixel respectively. Although the coherence image show high coherence in the Nea Kammeni island (the coherence in all other island is still low) no interfometric pattern deformation is recognized on it. Probably the temporal separation of the two acquisitions (211 days) is very short and so the amount of cumulate deformation in these 211 days was not detectable by the applied interferometric method. Furthermore with altitude of ambiguity of 84,79m, in the case of probable presence of one or two fringes the results is in the range of topographic error as the elevation of the island do not exceed 125m.

Concluding, the InSAR derived deformations, localized in Nea Kammeni island, revealed up to 6.2 cm of downlift. This measurement is significant as the volcano the last years is in rest condition. Taken in account the total deformation of 6.2 cm spanning a period of seven years we can assume that the average annual deformation is about 9 mm. In addition, this study show the capability to monitor with conventional InSAR ground deformation slowly accumulating in areas of interest, as Nea Kammeni is (low coherence), in conjunction with exceptional interferometric pairs in terms of baselines. Finally, a future application of more advanced interferometric techniques like the interferogram stacking [17] and PS interferometry [18] that overcomes some defects of the convetional interferometry, could reveal pattern of deformations also in the rest of the islands.

## ACKNOWLEDGEMENTS

The present study was carry out in the frame of ESA's Announcement of Opportunity for Greece and authors would like to thanks European Space Agency for the high level of collaboration and ERS and ENVISAT data provision.

## REFERENCES

[1] D. Massonnet and K.L. Feigl, "Radar interferometry and its application to changes in the earth's surface." Rev. Geophys., 36(4), pp.441-500, 1998.

[2] R.F. Hanssen, "Radar Interferometry. Data interpretation and Error Analysis," Kluwer Academic Publishers, Dordrecht, 2001.

[3] F. Amelung, D. Galloway, J. Bell, H. Zebker and R. Laczniak, "Sensing the ups and downs of Las Vegas: InSAR reveals structural control of land subsidence and aquifer-system Deformation," Geology, 27, 483-486, 1999.

[4] I. Parcharidis and E. Lagios, "Deformation in Nisyros Volcano (Greece) Using Differential Interferometry," Bull. Geol. Soc. Greece, 34/4, 1587-1594, 2001.

[5] F. Catani, P. Farina, S. Moretti, G. Nico and T. Strozzi, "On the application of SAR interferometry to geomorphological studies: Estimation of landform attributes and mass movements," Geomorphology, 66, pp. 119-131, 2005.

[6] C. Papavassiliou, K. Bostöm, S. Paritsis, V. Galanopoulos, N. Arvanitides and S. Kalogeropoulos, "Drilling of an ore-forming shallow hydrothermal system, Santorini volcano, Greece," Thera and the Aegean World III 2, Thera Foundation, London, pp. 250-256, 1990.

[7] M. Fytikas, O. Guiliani, F. Innocenti, G. Marinelli and R. Mazzuoli, "Geochronological data on recent magmatism of the Aegean Sea," Tectonophysics, 31, pp. 29-34, 1976.

[8] M. Fytikas, F. Innocenti, P. Manetti, R. Mazzuoli, A. Peccerilo and L. Villari, "Tertiary to Quaternary evolution of the volcanism in the Aegean region," In: J.E. Dixon and A.H.F. Robertson (eds.), The geological evolution of the eastern Mediterranean, Geol. Soc. London Spec. Pub., 17, pp. 687-699, 1984.

[9] C. Perissoratis, I. Angelopoulos and P. Zacharakis, "Petrographic description of marine sediments form Santorini: Evidence for a new submarine hot spring field in the bottom of the caldera," Thera and the Aegean World III 2, Thera Foundation, London, pp. 300-304,1990.

[10] K. Bostöm and N. Arvanitides, "The amount of exhalative-sedimentary deposits rich in Fe, Mn, P and Ba at Santorini," Bull. Geol. Soc. Greece, XXX/3, pp. 211-224, 1994.

[11] M. Fytikas, N. Kolios and G. Vougiokalakis, "Post-Minoan volcanic activity of the Santorini volcano, volcanic hazard and risk. Forecasting possibilities," Thera and the Aegean World III 2, Thera Foundation, London, pp. 183-198, 1990.

[12] H.Picher, D. Gunther and S. Kussmaul, Geological map of Greece, Thera Sheet, scale 1/50.000, I.G.M.E., Athens, 1980.

[13] C. Perissoratis, P. Zacharakis, S. Michailidis and E. Zimianitis, "Surficial sediment map of the Aegean sea floor," Santorini (Thira), Sheet 1, Scale 1/200000, I.G.M.E., Athens, 1995.
[14] H. Zebker and J. Villasenor, "Decorrelation in interferometric echoes," IEEE Transactions in Geoscience and Remote Sensing, 30, pp. 950-959, 1992.
[15] D. Massonet and K. Feigl, "Discriminating geophysical phenomena in satellite radar interferograms," Geophysical Research Letters, 22, pp. 1737-1740, 1995.
[16] R. Scharoo and P.N.A.M. Visser, "Precise orbit determination and gravity field improvement for the ERS satellites," Journal Geophysical Research, vol. 103, pp. 8113-8127, 1998.
[17] D. Raucoules, S. Le Mouélic, C. Carnec, C. Maisons and C.King, "Urban subsidence in the city of Prato (Italy) monitored by satellite radar interferometry," International Journal of Remote Sensing, vol. 24, n. 4, pp. 891-897, 2003.
[18] A. Ferretti, C. Prati and F. Rocca, "Permanent Scatterers in SAR Interferometry," IEEE Trans. on Geoscience and Remote Sensing, vol. 39, no. 1, pp. 8-20, 2001.